

1 Greenhouse gas fluxes in mangrove forest soil in an Amazon estuary

2 Saúl Edgardo Martínez Castellón^{1,2}, José Henrique Cattanio^{1,2*}, José Francisco
3 Berrêdo^{1,3,4}, Marcelo Rollnic^{3,2}, Maria de Lourdes Ruivo^{1,4,3}, Carlos Noriega^{3,2}.

4 ¹ Graduate Program in Environmental Sciences. Federal University of Pará, Belém,
5 Brazil

6 ² Biogeochemical Cycles Laboratory. Federal University of Pará, Belém, Brazil.

7 ^{2,3} Marine Environmental Monitoring Research Laboratory. Federal University of Pará,
8 Belém, Brazil.

9 ^{3,4} Department of Earth Sciences and Ecology. Paraense Emílio Goeldi Museum,
10 Belém, Brazil

11 * Corresponding author: cattanio@ufpa.br (J.H. Cattanio)

Formatado: Não Sobrescrito/
Subscrito

12 **Abstract:** Tropical mangrove forests are important carbon sinks, the soil being the
13 main carbon reservoir. Understanding the variability and the key factors that control
14 fluxes is critical to accounting for greenhouse gas (GHG) emissions, particularly in the
15 current scenario of global climate change. This study is the first to quantify carbon
16 dioxide (CO₂) and methane (CH₄) emissions using a dynamic chamber in a natural
17 mangrove soil of the Amazon. The plots for the trace gases study were allocated at
18 contrasting topographic heights. The results showed that the mangrove soil of the
19 Amazon estuary is a source of CO₂ (6.66 g CO₂ m⁻² d⁻¹) and CH₄ (0.13 g CH₄ m⁻² d⁻¹) to
20 the atmosphere. The CO₂ flux was higher in the high topography (7.86 g CO₂ m⁻² d⁻¹)
21 than in the low topography (4.73 g CO₂ m⁻² d⁻¹) in the rainy season, and CH₄ was higher
22 in the low topography (0.13 g CH₄ m⁻² d⁻¹) than in the high topography (0.01 g CH₄ m⁻²
23 d⁻¹) in the dry season. However, in the dry period, the low topography soil produced
24 more CH₄. Soil organic matter, carbon and nitrogen ratio (C/N), and redox potential
25 influenced the annual and seasonal variation of CO₂ emissions; however, they did not
26 affect CH₄ fluxes. The mangrove soil of the Amazon estuary produced 35.40 Mg CO_{2-eq}
27 ha⁻¹ y⁻¹. A total of 2.16 kg CO₂ m⁻² y⁻¹ needs to be sequestered by the mangrove
28 ecosystem to counterbalance CH₄ emissions.

Formatado: Fonte: Negrito

29 1 Introduction

30 Mangrove areas are estimated to be the main contributors to greenhouse gas emissions
31 in marine ecosystems (Allen et al., 2011; Chen et al., 2012). However, mangrove forests
32 are highly productive due to a high nutrient turnover rate (Robertson et al., 1992) and
33 have mechanisms that maximize carbon gain and minimize water loss through plant
34 transpiration (Alongi and Mukhopadhyay, 2015). A study conducted in 25 mangrove
35 forests (between 30° latitude and 73° longitude) revealed that these forests are the

36 richest in carbon (C) storage in the tropics, containing on average 1,023 Mg C ha⁻¹ of
37 which 49 to 98% is present in the soil (Donato et al., 2011).

38 The estimated soil CO₂ flux in tropical estuarine areas is 16.2 Tg C y⁻¹ (Alongi, 2009).
39 However, soil efflux measurements from tropical mangroves revealed emissions
40 ranging from 2.9 to 11.0 g CO₂ m⁻² d⁻¹ (Castillo et al., 2017; Chen et al., 2014; Shiau
41 and Chiu, 2020). In situ CO₂ production is related to the water input of terrestrial,
42 riparian, and groundwater brought by rainfall (Rosentreter et al., 2018b). Due to the
43 periodic tidal movement, the mangrove ecosystem is daily flooded, leaving the soil
44 anoxic and consequently reduced, favoring methanogenesis (Dutta et al., 2013). Thus,
45 estuaries are considered hotspots for CH₄ production and emission (Bastviken et al.,
46 2011; Borges et al., 2015). Organic material decomposition by methanogenic bacteria in
47 anoxic environments, such as sediments, inner suspended particles, zooplankton gut
48 (Reeburgh, 2007; Valentine, 2011), and the impact of freshwater should change the
49 electron flow from sulfate-reducing bacteria to methanogenesis (Purvaja et al., 2004),
50 which also results in CH₄ formation. On the other hand, high salinity levels, above 18
51 ppt, may result in an absence of CH₄ emissions (Poffenbarger et al., 2011), since CH₄
52 dissolved in pores is typically oxidized anaerobically by sulfate (Chuang et al., 2016).
53 Currently the uncertainty in emitted CH₄ values in vegetated coastal wetlands is
54 approximately 30% (EPA, 2017). Soil flux measurements from tropical mangroves
55 revealed emissions range from 0.3 to 4.4 mg CH₄ m⁻² d⁻¹ (Castillo et al., 2017; Chen et
56 al., 2014; Kreuzwieser et al., 2003).

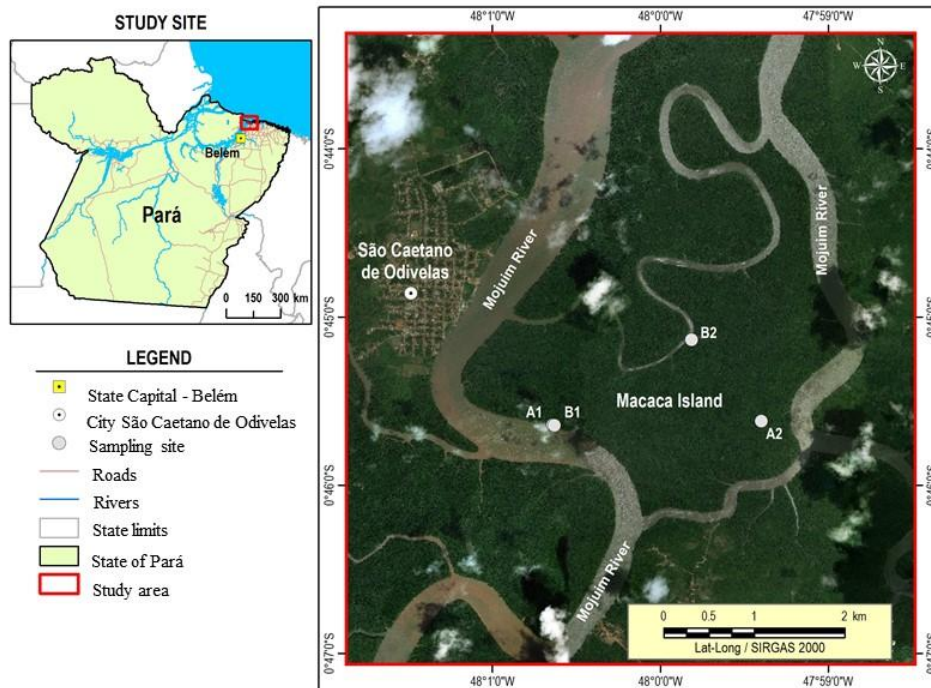
57 The production of greenhouse gases from soils is mainly driven by biogeochemical
58 processes. Microbial activities and gas production are related to soil properties,
59 including total carbon and nitrogen concentrations, moisture, porosity, salinity, and
60 redox potential (Bouillon et al., 2008; Chen et al., 2012). Due to the dynamics of tidal
61 movements, mangrove soils may become saturated and present reduced oxygen
62 availability, or suffer total aeration caused by the ebb tide. Studies attribute soil carbon
63 flux responses to moisture perturbations because of seasonality and flooding events
64 (Banerjee et al., 2016), with fluxes being dependent on tidal extremes (high tide and low
65 tide), and flood duration (Chowdhury et al., 2018). In addition, phenolic compounds
66 inhibit microbial activity and help keep organic carbon intact, thus leading to the
67 accumulation of organic matter in mangrove forest soils (Friesen et al., 2018).

68 The Amazonian coastal areas in the State of Pará (Brazil) cover 2,176.8 km² where
69 mangroves develop under the macro-tide regime (Souza Filho, 2005), representing
70 approximately 85% of the entire area of Brazilian mangroves (Herz, 1991). The
71 objective of this study is to investigate the monthly flux of CO₂ and CH₄ from the soil,
72 at two topographic heights, in a pristine mangrove area in the Mojuim River Estuary,
73 belonging to the Amazon biome. The gas fluxes were studied together with the analysis
74 of the vegetation structure and soil physical-chemical parameters.

75 **2 Material and Methods**

76 **2.1 Study site**

77 This study was conducted in the Amazonian coastal zone, Macaca Island (-0.746491
78 latitude and -47.997219 longitude), located in the Mojuim River estuary, at the
79 Mocapajuba Marine Extractive Reserve, municipality of São Caetano de Odivelas
80 (Figure-Fig. 1), state of Pará (Brazil). The Macaca island has an area of 1,322 ha of
81 pristine mangroves, and belongs to a mangrove area of 2,177 km² in the state of Pará
82 (Souza Filho, 2005). The climate is type Am (tropical monsoon) according to the
83 Köppen classification (Peel et al., 2007). The climatological data were obtained from
84 the Meteorological Database for Teaching and Research of the National Institute of
85 Meteorology (INMET). The area has a rainy season from January to June (2,296 mm of
86 precipitation) and a dry season from July to December (687 mm). March and April were
87 the rainiest months with 505 and 453 mm of precipitation, while October and November
88 were the driest (53 and 61 mm, respectively). The minimum temperatures occur in the
89 rainy period (26 °C) and the maximum in the dry period (29 °C). The Mojuim estuary
90 has a macrotidal regime, with an average amplitude of 4.9 m during spring tide and 3.2
91 m during low tide (Rollnic et al., 2018). During the wet season the Mojuim River has a
92 flow velocity of 1.8 m s⁻¹ at the ebb tide and 1.3 m s⁻¹ at the flood tide, whereas in the
93 dry season, the maximum currents reach 1.9 m s⁻¹ at the flood and 1.67 m s⁻¹ at the ebb
94 tide (Rocha, 2015). The annual mean salinity of the river water is 26.95 PSU (Valentim
95 et al., 2018).



Formatado: Fonte: Negrito

96

97 **Figure 1.** The Macaca Island located in the mangrove coast of Northern Brazil,
 98 Municipality of São Caetano de Odivelas (state of Pará), with sampling points at low
 99 (plot B1 and plot B2) and high (plot A1 and plot A2) topographies. Image Source: ©
 100 Google Earth

101 The Mojuim River region is geomorphologically formed by partially submerged river
 102 basins consequent of the increase in the relative sea level during the Holocene (Prost et
 103 al., 2001) associated with the formation of mangroves, dunes, and beaches (El-Robrini
 104 et al., 2006). Before reaching the estuary, the Mojuim River crosses an area of a dryland
 105 forest highly fragmented by family farming, forming remnants of secondary forest (<
 106 5.0 ha) of various ages (Fernandes and Pimentel, 2019). The population economically
 107 exploited the estuary, primarily by artisanal fishing, crab (*Ucides cordatus* L.)
 108 extraction, and oyster farms.

109 The flora of the mangrove area of Macaca Island is little anthropized and comprises the
 110 plant genera *Rhizophora*, *Avicenia*, *Laguncularia*, and *Acrostichum* (Ferreira, 2017;
 111 França et al., 2016). The estuarine plains are influenced by macrotide dynamics and can
 112 be physiographically divided into four sectors according to the different vegetation
 113 covers, associated with the landforms distribution, topographic gradient, tidal

114 inundation, and levels of anthropic transformation (França et al., 2016). The Macaca
115 Island is ranked as being from the fourth sector, which implies having woods of adult
116 trees of the genus *Ryzophora* with an average height of 10 to 25 m, is located at an
117 elevation of 0 to 5 m, and having silt-clay soil (França et al., 2016).

118 | Four sampling plots were selected in the Macaca Island (Figure-Fig. 1) on 19/05/2017,
119 | when the moon was in the waning quarter phase: two plots where flooding occurs every
120 | day (plots B1 and B2; Figure-Fig. 1), called low topography (Top_Low), and two plots
121 | where flooding occurs only at high tides during the solstice and on the high tides of the
122 | rainy season of the new and full moons (plots A1 and A2; Figure-Fig. 1), called high
123 | topography (Top_High).

124 **2.2 Greenhouse gas flux measurements**

125 In each plot, eight Polyvinyl Chloride rings with 0.20 m diameter and 0.12 m height
126 were randomly installed within a circumference with a diameter of 20 m. The rings had
127 an area of 0.028 m² (volume of 3.47 L), were fixed 0.05 m into the ground, and
128 remained in place until the study was completed. Once a month, gas fluxes were
129 measured during periods of waning or crescent moon, as these are the times when the
130 soil in the low topography is more exposed. To avoid the influence of mangrove roots
131 on the gas fluxes, the rings were placed in locations without any seedlings or
132 aboveground mangrove roots. The CO₂ and CH₄ concentrations (ppm) were measured
133 using the dynamic chamber methodology (Norman et al., 1997; Verchot et al., 2000),
134 sequentially connected to a Los Gatos Research portable gas analyzer (Mahesh et al.,
135 2015). The device was calibrated monthly with a high quality standard gas (500 ppm
136 CO₂; 5 ppm CH₄). The rings were sequentially closed for three minutes with a PVC cap,
137 being connected to the analyzer through two 12.0 m polyethylene hoses. The gas
138 concentration was measured every two seconds and automatically stored by the
139 analyzer. CO₂ and CH₄ fluxes were calculated from the linear regression of
140 increasing/decreasing CO₂ and CH₄ concentrations within the chamber, usually between
141 one and three minutes after the ring cover was placed (Frankignoulle, 1988; McEwing
142 et al., 2015). The flux is considered zero when the linear regression reaches an R² <
143 0.30 (Sundqvist et al., 2014). However, in our analyses, most regressions reached R² >
144 0.70, and the regressions were weak and considered zero in only 6% of the samples. At
145 the end of each flux measurement, the height of the ring above ground was measured at

146 four equidistant points with a ruler. The seasonal data were analyzed by comparing the
147 average monthly fluxes in the wet season and dry season separately.

148 **2.3 Vegetation structure and biomass**

149 The floristic survey was conducted in October 2017 using circular 1,256.6 m² plots
150 (Kauffman et al., 2013) divided into four 314.15 m² subplots, which is the equivalent to
151 0.38 ha, at the same topographies as the gas flux analysis (Figure-Fig. 1). We recorded
152 the diameter above the aerial roots, the diameter of the stem, and total height of all trees
153 with DBH (diameter at breast height; m) greater than 0.05m. The allometric equations
154 (Howard et al., 2014) to calculate tree biomass (aboveground biomass; AGB) were:
155 $AGB = 0.1282 * DBH^{2.6}$ ($R^2 = 0.92$) for *R. mangle*; $AGB = 0.140 * DBH^{2.4}$ ($R^2 = 0.97$)
156 for *A. germinans*; and $Total\ AGB = 0.168 * \rho * DBH^{2.47}$ ($R^2 = 0.99$), where $\rho_{R. mangle} =$
157 0.87 ; $\rho_{A. germinans} = 0.72$ ($\rho =$ wood density).

158 **2.4 Soil sampling and environmental characterization**

159 Four soil samples were collected with an auger at a depth of 0.10 m in all the studied
160 plots for gas flux measurements (Figure-Fig. 1) in July 2017 (beginning of the dry
161 season) and January 2018 (beginning of the rainy season). Before the soil samples were
162 removed, pH and redox potential (Eh; mV) were measured with a Metrohm 744
163 equipment by inserting the platinum probe directly into the intact soil at a depth of 0.10
164 m (Bauza et al., 2002). The soil samples collected in the field were transported to the
165 laboratory (Chemical Analysis Laboratory of the *Museu Paraense Emílio Goeldi*) in
166 thermal boxes containing ice. The soil samples were analyzed on the day after collection
167 at the laboratory, and the samples were kept in a freezer. Salinity (Sal; ppt) was
168 measured with PCE-0100, and soil moisture (Sm; %) by the residual gravimetric
169 method (EMBRAPA, 1997).

170 Organic Matter (OM; g kg⁻¹), Total Carbon (T_C; g kg⁻¹) and Total Nitrogen (T_N; g kg⁻¹)
171 were calculated by volumetry (oxidoreduction) using the Walkley-Black method
172 (Kalembasa and Jenkinson, 1973). Microbial carbon (C_{mic}; mg kg⁻¹) and microbial
173 nitrogen (N_{mic}; mg kg⁻¹) were determined through the 2.0 min of Irradiation-extraction
174 method of soil by microwave technique (Islam and Weil, 1998). Microwave heated soil
175 extraction proved to be a simple, fast, accurate, reliable, and safe method to measure
176 soil microbial biomass (Araujo, 2010; Ferreira et al., 1999; Monz et al., 1991). The C_{mic}
177 was determined by dichromate oxidation (Kalembasa and Jenkinson, 1973; Vance et al.,

178 1987). The N_{mic} was analyzed following the method described by Brookes et al. (1985),
179 changing fumigation to irradiation, which uses the difference between the amount of T_N
180 in irradiated and non-irradiated soil. We used the flux conversion factor of 0.33
181 (Sparling and West, 1988) and 0.54 (Almeida et al., 2019; Brookes et al., 1985), for
182 carbon and nitrogen, respectively. Particle size analysis was performed separately on
183 four soil samples collected at each flux plot, in the two seasons (October 2017 and
184 March 2018), according to EMBRAPA (1997).

185 At each gas flux measurement, environmental variables such as air temperature (T_{air} ,
186 °C), relative humidity (RH, %), and wind speed (W_s , $m\ s^{-1}$) were quantified with a
187 portable thermo-hygrometer (model AK821) at the height of 2.0 m above the soil
188 surface. Soil temperature (T_s , °C) was measured with a portable digital thermometer
189 (model TP101) after each gas flux measurement. Daily precipitation was obtained from
190 an automatic precipitation station installed at a pier on the banks of the Mojuim River in
191 São Caetano das Odivelas (coordinates: -0.738333 latitude; -48.013056 longitude).

192 **2.5 Statistical analyses**

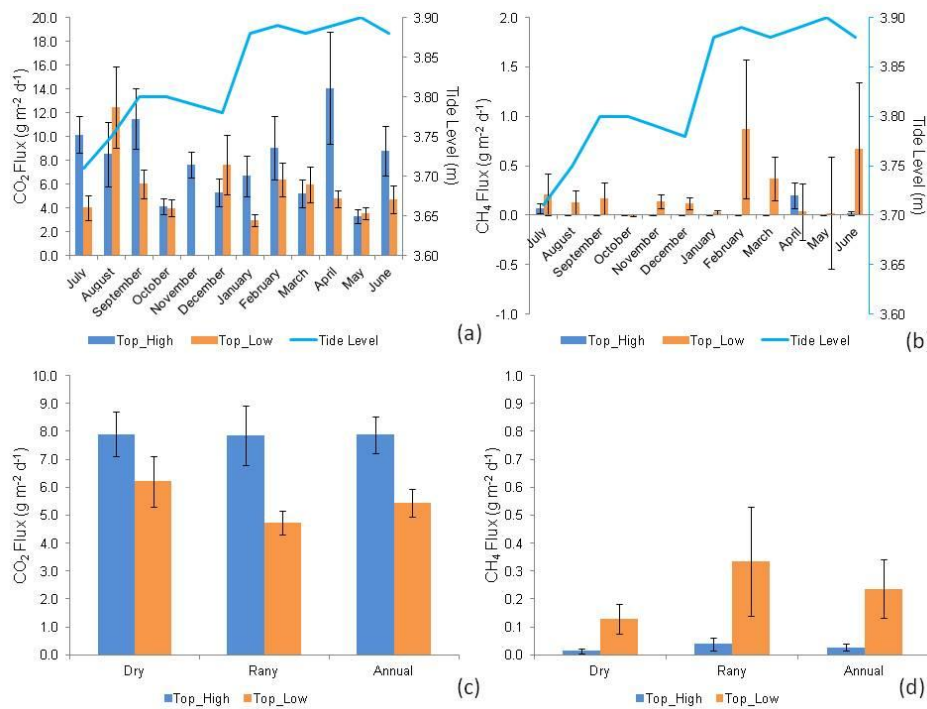
193 On the Macaca Island, two treatments were allocated (low and high topography), with
194 two plots in either treatment. In each plot, eight chambers were randomly distributed,
195 which were considered sample repetitions. The normality of the data of CH_4 and FCO_2
196 flux, and soil physicochemical parameters was evaluated using the Shapiro-Wilks
197 method. The soil CO_2 and CH_4 flux showed a non-normal distribution. Therefore, we
198 used the non-parametric ANOVA (Kruskal-Wallis, $p < 0.05$) to test the differences
199 between the two treatments among months and seasons. The physicochemical
200 parameters were normally distributed. Therefore, a parametric ANOVA was used to test
201 the statistical differences ($p < 0.05$) between the two treatments among months and
202 seasons. Pearson correlation coefficients were calculated to determine the relationships
203 between soil properties and gas fluxes in the months (dry and wet season) when the
204 chemical properties of the soil were analyzed at the same time as gas fluxes were
205 measured. Statistical analyses were performed with the free statistical software Infostat
206 2015®.

207 **3 Results**

208 **3.1 Carbon dioxide and methane fluxes**

209 CO₂ fluxes differed significantly between topographies only in January (H = 3.915; p =
 210 0.048), July (H = 9.091; p = 0.003), and November (H = 11.294; p < 0.001) (Figure-Fig.
 211 2; Supplementary Information, SI 1), with generally higher fluxes at the high
 212 topography than at the low topography. At the high topography, CO₂ fluxes were
 213 significantly higher (H = 24.510; p = 0.011) in July compared to August and December,
 214 March, October, and May, not differing from the other months of the year. Similarly, at
 215 the low topography, CO₂ fluxes were statistically significantly higher (H = 19.912; p =
 216 0.046) in September and February ~~than in~~ when compared to January and November, not
 217 differing from the other months. We found a mean monthly flux of 7.9 ± 0.7 g CO₂ m⁻²
 218 d⁻¹ (mean \pm standard error) and 5.4 ± 0.5 g CO₂ m⁻² d⁻¹ at the high and low
 219 topographies, respectively.

220



221

222 **Figure 2.** CO₂ (a) and CH₄ (b) fluxes (g CO₂ or CH₄ m⁻² d⁻¹) monthly (July 2018 to
 223 June 2019) (n = 16). Seasonal (Dry and Rainy) and annual fluxes of CO₂ (c) and CH₄

Formatado: Fonte: Negrito

224 (d), at high (Top_High) and low (Top_Low) topographies (n = 96), in a mangrove forest
225 soil compared to tide level (Tide Level). The bars represent the standard error of the
226 mean.

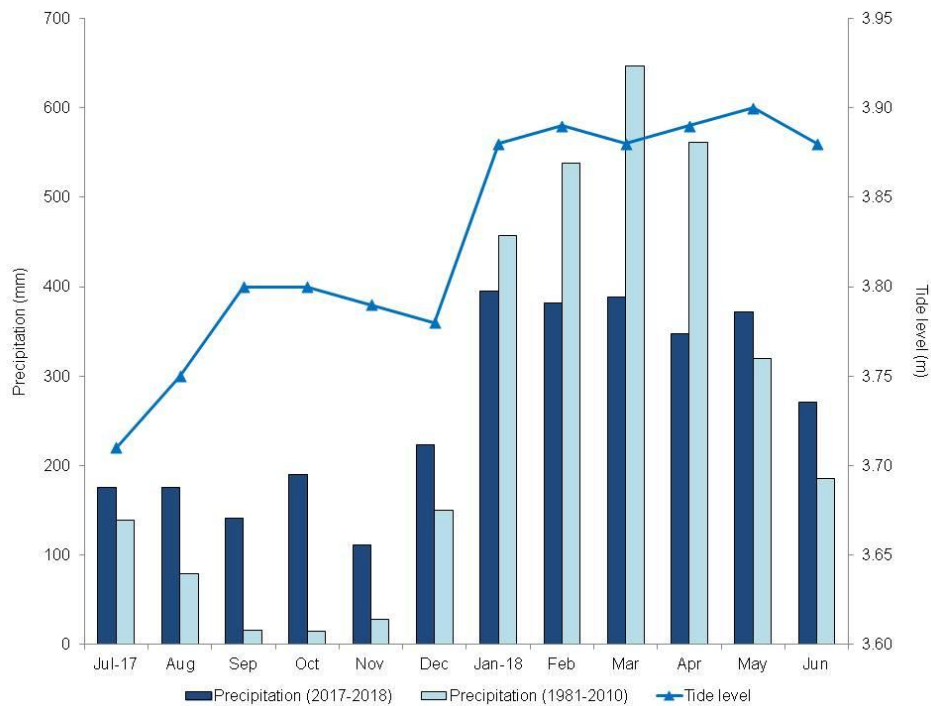
227 The CH₄ fluxes were statistically different between topographies only in November (H
228 = 9.276; p = 0.002) and December (H = 4.945; p = 0.005), with higher fluxes at the low
229 topography (Figure-Fig. 2; SI 1). At the high topography, CH₄ fluxes were significantly
230 (H = 40.073; p < 0.001) higher in April and July compared to the other months studied,
231 and in November CH₄ was consumed from the atmosphere (Figure-Fig. 2; SI 1).
232 Similarly, CH₄ fluxes at the low topography did not vary significantly among months
233 (H = 10.114; p = 0.407).

234 Greenhouse gas fluxes (Figure-Fig. 2) were only significantly different between
235 topographies in the dry season (Figure-Fig. 3), period when CO₂ fluxes were higher (H
236 = 7.378; p = 0.006) at the high topography and CH₄ fluxes at the low topography (H =
237 8.229; p < 0.001). In the Macaca Island, the mean annual fluxes of CO₂ and CH₄ were
238 6.659 ± 0.419 g CO₂ m⁻² d⁻¹ and 0.132 ± 0.053 g CH₄ m⁻² d⁻¹, respectively. During the
239 study year, the CO₂ flux from the mangrove soil ranged from -5.06 to 68.96 g CO₂ m⁻²
240 d⁻¹ (mean 6.66 g CO₂ m⁻² d⁻¹), while the CH₄ flux ranged from -5.07 to 11.08 g CH₄ m⁻²
241 d⁻¹ (mean 0.13 g CH₄ m⁻² d⁻¹), resulting in a total carbon efflux rate of 1.92 g C m⁻² d⁻¹
242 or 7.00 Mg C ha⁻¹ y⁻¹ (Figure-Fig. 2).

243 3.2 Weather data

244 There was a marked seasonality during the study period (Figure-Fig. 2), with 2,155.0
245 mm of precipitation during the rainy period and 1,016.5 mm during the dry period. The
246 highest tides occurred in the period of greater precipitation (Figure-Fig. 3) due to the
247 rains. However, the rainfall distribution was different from the climatological normal
248 (Figure-Fig. 3). The precipitation in the rainy season was 553.2 mm below and in the
249 dry season was 589.1 mm above the climatological normal. Thus, in the period studied,
250 the dry season was rainier and the rainy season drier than the climatological normal,
251 which may be a consequence of the La Niña event (Wang et al., 2019).

252

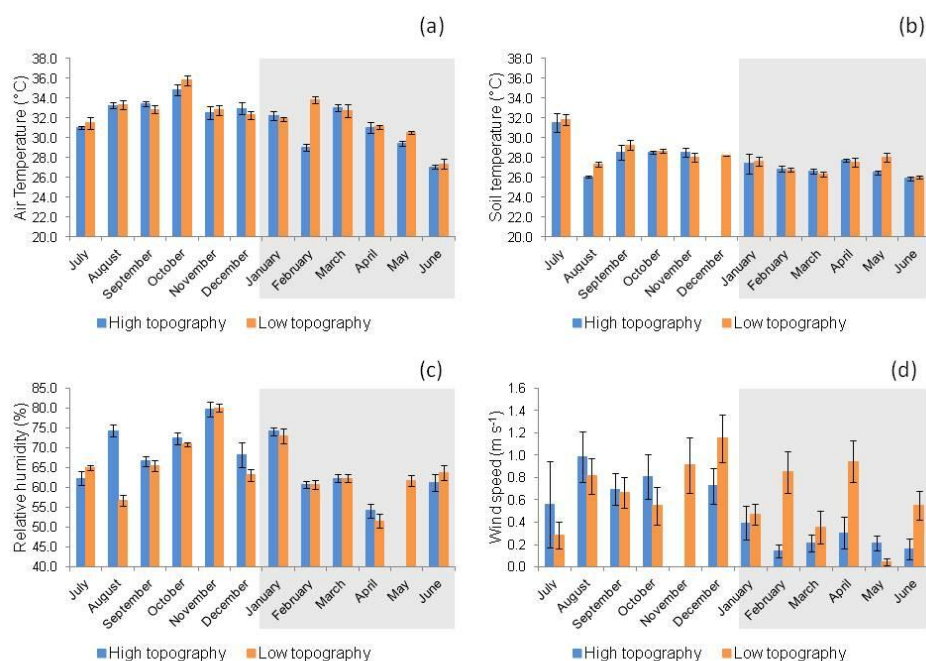


253

254 **Figure 3.** Monthly climatological normal in the municipality of Soure (1981-2010,
 255 mm), monthly precipitation (mm), and maximum tide height (m) from 2017 to 2018, in
 256 the municipality of São Caetano de Odivelas (PA).

Formatado: Fonte: Negrito

257 T_{air} was significantly higher (LSD = 0.72, $p = 0.01$) at the high (31.24 ± 0.26 °C) than at
 258 the low topography (30.30 ± 0.25 °C) only in the rainy season (Figure-Fig. 4a). No
 259 significant variation in T_s was found between topographies in either season (Figure-Fig.
 260 4b). RH was significantly higher (LSD = 2.55, $p = 0.01$) at the high topography ($70.54 \pm$
 261 0.97%) than at the low topography ($66.85 \pm 0.87\%$) only in the rainy season (Figure
 262 Fig. 4c). W_s (Figure-Fig. 4d) was significantly higher (LSD = 0.15, $p < 0.00$) at the low
 263 (0.54 ± 0.06 m s⁻¹) than at the high topography (0.24 ± 0.04 m s⁻¹) also in the rainy
 264 season.



265

266 | **Figure 4.** a) Air temperature (°C), b) soil temperature (°C), c) relative humidity (%),
 267 and d) wind speed (m s⁻¹) at high and low topographies, from July 2017 to June 2018 in
 268 a mangrove area in the Mojuim River estuary. Bars highlighted in grey correspond to
 269 the rainy season (n = 16). The bars represent the standard error.

Formatado: Fonte: Negrito

270 3.3 Soil characteristics

271 Silt concentration was higher at the low topography (LSD: 14.763; p= 0.007) and clay
 272 concentration was higher at the high topography plots (LSD: 12.463; p= 0.005), in both
 273 seasons studied (Table 1). Soil particle size analysis did not differ statistically (p > 0.05)
 274 between the two seasons (Table 1). Soil moisture did not vary significantly (p > 0.05)
 275 between topographies at each season, or between seasonal periods at the same
 276 topography (Table 1). The pH varied statistically (LSD: 5.950; p= 0.006) only at the
 277 low topography when the two seasons were compared, being more acidic in the dry
 278 period (Table 1). The pH values were significantly (LSD: 0.559; p= 0.008) higher in the
 279 dry season (Table 1). No variation in Eh was identified between topographies and
 280 seasons (Table 1), although it was higher in the dry season than in the rainy season.
 281 However, Sal values were higher (LSD: 3.444; p = 0.010) at the high topography than at
 282 the low topography in the dry season (Table 1). In addition, Sal was significantly higher

283 in the dry season than in the rainy season, in both high (LSD: 2.916; $p < 0.001$) and low
284 (LSD: 3.003; $p < 0.001$) topographies (Table 1).

285 **Table 1.** Analysis of Sand (%), Silt (%), Clay (%), Moisture (%), pH, Redox Potential (Eh, mV) and salinity (Sal; ppt) in the mangrove soil of
 286 high and low topographies, and in the rainy and dry seasons (Macaca island, São Caetano das Odivelas). Numbers represent the mean \pm standard
 287 error of the mean. Lower case letters compare topographies in each seasonal period and upper-case letters compare the same topography between
 288 seasonal periods. Different letters indicate statistical difference (LSD, $p < 0.05$).

Formatado: Fonte: Negrito

Season	Topography	Sand (%)	Silt (%)	Clay (%)	Moisture (%)	pH	Eh (mV)	Sal (ppt)
Dry	High	12.1 \pm 1.4 ^{aA}	41.8 \pm 3.3 ^{bA}	46.1 \pm 2.6 ^{aA}	73.1 \pm 6.6 ^{aA}	5.5 \pm 0.2 ^{aA}	190.25 \pm 45.53 ^{aA}	35.25 \pm 1.11 ^{aA}
	Low	9.7 \pm 2.5 ^{aA}	63.6 \pm 6.1 ^{aA}	26.6 \pm 5.2 ^{bA}	86.9 \pm 3.4 ^{aA}	5.3 \pm 0.3 ^{aA}	106.38 \pm 53.76 ^{aA}	30.13 \pm 1.16 ^{bA}
	Mean	10.9 \pm 1.4 ^A	52.7 \pm 4.4 ^A	36.4 \pm 3.8 ^A	80.0 \pm 4.0 ^A	5.4 \pm 0.2 ^A	148.31 \pm 35.71 ^A	32.69 \pm 1.02 ^A
Rainy	High	12.3 \pm 1.0 ^{aA}	39.3 \pm 2.1 ^{bA}	48.4 \pm 1.6 ^{aA}	88.9 \pm 3.5 ^{aA}	4.9 \pm 0.4 ^{aA}	92.50 \pm 56.20 ^{aA}	7.50 \pm 0.78 ^{aB}
	Low	7.8 \pm 1.4 ^{bA}	63.4 \pm 5.2 ^{aA}	28.8 \pm 4.2 ^{bA}	88.6 \pm 3.7 ^{aA}	4.4 \pm 0.1 ^{aB}	36.25 \pm 49.97 ^{aA}	8.13 \pm 0.79 ^{aB}
	Mean	10.1 \pm 1.1 ^A	51.4 \pm 4.1 ^A	38.6 \pm 3.4 ^A	88.7 \pm 2.5 ^A	4.6 \pm 0.2 ^B	64.38 \pm 37.04 ^A	7.81 \pm 0.54 ^B

289

290 The C_{mic} did not differ between topographies in the two seasons (Table 2). However, T_C
291 was significantly higher in the low topography in the dry season (LSD: 5.589; $p <$
292 0.000) and in the rainy season (LSD: 5.777; $p = 0.024$). In addition, C_{mic} was higher in
293 the dry season in both the high (LSD: 11.325; $p < 0.010$) and low (LSD: 9.345; $p <$
294 0.000) topographies (Table 2). N_{mic} did not vary between topographies seasonally.
295 However, N_{mic} in the high (LSD: 9.059; $p = 0.013$) and low topographies (LSD: 4.447;
296 $p = 0.001$) was higher during the dry season (Table 2). The C/N ratio (Table 2) was
297 higher in the low than in the high topography in both the dry (LSD: 3.142; $p < 0.000$)
298 and rainy seasons (LSD: 3.675; $p = 0.033$). However, only in the low topography was
299 the C/N ratio higher (LSD: 1.863; $p < 0.000$) in the dry season than in the rainy season
300 (Table 2). Soil OM was higher at the low topography in the rainy (LSD: 9.950; $p <$
301 0.024) and in the dry seasons (LSD: 9.630; $p < 0.000$). Only in the lowland topography
302 was the OM concentration higher in the dry season than in the rainy season (Table 2).

303 **Table 2.** Seasonal and topographic variation in microbial Carbon (C_{mic} ; $mg\ kg^{-1}$), microbial Nitrogen (N_{mic} ; $mg\ kg^{-1}$), Total Carbon (T_C ; $g\ kg^{-1}$),
 304 Total Nitrogen (N_T ; $g\ kg^{-1}$), Carbon/Nitrogen ratio (C/N) and Soil Organic Matter (OM; $g\ kg^{-1}$). Numbers represent the mean (\pm standard error).
 305 Lower case letters compare topographies at each season, and upper-case letters compare the topography between seasons.

Formatado: Fonte: Negrito

Season	Topography	C_{mic} $mg\ kg^{-1}$	N_{mic} $mg\ kg^{-1}$	T_C $g\ kg^{-1}$	T_N $g\ kg^{-1}$	C/N	OM $g\ kg^{-1}$
Dry	High	22.12 \pm 5.22 ^{aA}	12.76 \pm 4.20 ^{aA}	14.12 \pm 2.23 ^{bA}	1.43 \pm 0.06 ^{aA}	9.60 \pm 1.20 ^{bA}	24.35 \pm 3.84 ^{bA}
	Low	26.34 \pm 4.23 ^{aA}	10.34 \pm 2.05 ^{aA}	26.44 \pm 1.35 ^{aA}	1.56 \pm 0.04 ^{aA}	16.98 \pm 0.84 ^{aA}	45.59 \pm 2.32 ^{aA}
	Mean	24.23 \pm 3.29 ^A	11.55 \pm 2.28 ^A	20.28 \pm 2.03 ^A	1.49 \pm 0.04 ^A	13.29 \pm 1.19 ^A	34.97 \pm 3.50 ^A
Rainy	High	7.40 \pm 0.79 ^{aB}	0.75 \pm 0.41 ^{aB}	11.46 \pm 2.48 ^{bA}	1.32 \pm 0.04 ^{aA}	8.42 \pm 1.70 ^{bA}	19.75 \pm 4.27 ^{bA}
	Low	5.95 \pm 1.06 ^{aB}	1.23 \pm 0.28 ^{aB}	18.27 \pm 1.06 ^{aB}	1.46 \pm 0.06 ^{aA}	12.47 \pm 0.22 ^{aB}	31.51 \pm 1.83 ^{aB}
	Mean	6.68 \pm 0.67 ^B	0.99 \pm 0.25 ^B	14.86 \pm 1.57 ^B	1.39 \pm 0.04 ^A	10.44 \pm 0.98 ^A	25.63 \pm 2.71 ^B

306

307 **3.4 Vegetation structure and biomass**

308 Only the species *R. mangle* and *A. germinans* were found in the floristic survey carried
309 out. The DBH did not vary significantly between the topographies for either species
310 (Table 3). However, *R. mangle* had a higher DBH than *A. germinaris* at both high
311 (LSD: 139.304; $p = 0.037$) and low topographies (LSD: 131.307; $p = 0.001$). The basal
312 area (BA) and AGB did not show significant variation (Table 3). A total aboveground
313 biomass of $322.1 \pm 49.6 \text{ Mg ha}^{-1}$ was estimated.

314

315 **Table 3.** Summed Diameter at Breast Height (DBH; cm), Basal Area (BA; m² ha⁻¹) and Aboveground Biomass (AGB; Mg ha⁻¹) at high and low
 316 topographies in the mangrove forest of the Mojuim River estuary. Numbers represent the mean ± standard error of the mean. Lower case letters
 317 compare topographic height for each species, and upper-case letters compare species at each topographic height, using Tukey's test (p < 0.05).

Formatado: Fonte: Negrito

Specie	Topography	N ha ⁻¹	DBH (cm)	BA (m ² ha ⁻¹)	AGB (Mg ha ⁻¹)
<i>Rhizophora</i>	High	302.4±20.5	238.8±24.9 ^{aA}	17.3±2.0 ^{aA}	219.3±25.7 ^{aA}
<i>mangle</i>	Low	310.4±37.6	283.5±45.0 ^{aA}	24.2±4.3 ^{aA}	338.7±62.9 ^{aA}
<i>Avicennia</i>	High	47.7±20.5	86.8±51.2 ^{aB}	13.8±9.2 ^{aA}	135.3±94.7 ^{aA}
<i>germinans</i>	Low	15.9±9.2	46.1±29.3 ^{aB}	11.8±8.8 ^{aA}	136.0±108.3 ^{aA}
Total	High	350.2±18.4	325.6±33.6 ^a	31.1±7.5 ^a	304.5±99.8 ^a
	Low	346.2±41.0	296.0±23.7 ^a	30.0±4.1 ^a	330.8±60.4 ^a

318 The equations for biomass estimates (AGB) were: *R. mangle* = 0.1282*DBH^{2.6}; *A. germinans* = 0.14*DBH^{2.4}; and Total = 0.168*ρ*DBH^{2.47}, where ρ_{*R. mangle*} = 0.87; ρ_{*A. germinans*}
 319 = 0.72 (Howard et al., 2014).

320 **3.5 Drivers of greenhouse gas fluxes**

321 In the rainy season, CO₂ efflux was correlated with T_{air} (Pearson = 0.23, p = 0.03), RH
322 (Pearson = -0.32, p < 0.00) and T_s (Pearson = 0.21, p = 0.04) only at the low
323 topography. In the dry season CO₂ flux was correlated with T_s (Pearson = 0.39, p <
324 0.00) at the low topography. The dry season was the period in which we found the
325 greatest amount of significant correlations between CO₂ efflux and soil chemical
326 parameters, while the C:N ratio, OM, and Eh were correlated with CO₂ efflux in both
327 seasons (Table 4). The negative correlation between T_C, N_T, C/N, and OM, along with
328 the positive correlation of N_{mic} with soil CO₂ flux, in the dry period, indicates that
329 microbial activity is a decisive factor for CO₂ efflux (Table 4). Soil moisture in the
330 Mojuim River mangrove forest negatively influenced CO₂ flux in both seasons (Table
331 4). However, soil moisture was not correlated with CH₄ flux. No significant correlations
332 were found between CH₄ efflux and the chemical properties of the soil in the mangrove
333 of the Mojuim River estuary (Table 4).

334

335 **Table 4.** Correlation coefficient (Pearson) of CO₂ and CH₄ fluxes with chemical parameters of the soil in a mangrove area in the Mojuim River
 336 estuary.

Formatado: Fonte: Negrito

Gas Flux (g m ⁻² d ⁻¹)	Season	T _C (g kg ⁻¹)	T _N (g kg ⁻¹)	C _{mic} (mg kg ⁻¹)	N _{mic} (mg kg ⁻¹)	C/N	OM (g kg ⁻¹)	Sal (ppt)	Eh (mV)	pH	Moisture (%)
CO ₂	Dry	-0.68**	-0.59*	0.18 ^{NS}	0.61**	-0.66**	-0.67**	-0.07 ^{NS}	0.51*	0.21 ^{NS}	-0.49*
	Rainy	-0.44 ^{NS}	-0.20 ^{NS}	-0.15 ^{NS}	-0.32 ^{NS}	-0.50*	-0.63**	-0.54*	0.53*	0.47 ^{NS}	-0.54*
	Annual	-0.50**	-0.35*	-0.18 ^{NS}	0.00 ^{NS}	-0.53**	-0.48**	-0.30 ^{NS}	0.39*	0.23 ^{NS}	-0.56**
CH ₄	Dry	0.30 ^{NS}	0.07 ^{NS}	-0.14 ^{NS}	-0.24 ^{NS}	0.34 ^{NS}	0.02 ^{NS}	-0.04 ^{NS}	-0.38 ^{NS}	0.26 ^{NS}	0.26 ^{NS}
	Rainy	0.05 ^{NS}	-0.09 ^{NS}	0.44 ^{NS}	-0.27 ^{NS}	0.09 ^{NS}	-0.11 ^{NS}	-0.04 ^{NS}	-0.13 ^{NS}	-0.07 ^{NS}	0.04 ^{NS}
	Annual	0.04 ^{NS}	-0.10 ^{NS}	-0.01 ^{NS}	-0.18 ^{NS}	0.08 ^{NS}	-0.01 ^{NS}	-0.17 ^{NS}	-0.21 ^{NS}	-0.08 ^{NS}	0.02 ^{NS}

337 Total Carbon (T_C; g kg⁻¹); Total Nitrogen (T_N; g kg⁻¹); Microbial Carbon (C_{mic}, g kg⁻¹); Microbial Nitrogen (N_{mic}, g kg⁻¹); Carbon and Nitrogen
 338 ratio (C/N); Organic Matter (OM; g kg⁻¹); Salinity (Sal; ppt); Redox Potential (Eh; mV); Soil Moisture (Moisture, %).

339 NS= not significant; * significant effects at p ≤ 0.05; ** significant effects at p ≤ 0.01

340

341 4 Discussion

342 4.1 Carbon dioxide and methane flux

343 It is important to consider that the year under study was rainier in the dry season (2017)
344 and less rainy in the wet season (2018) when the climatological average is concerned
345 (1981-2010) (~~Figure-Fig.~~ 3). Perhaps this variation is related to the La Niña effects
346 (~~extreme event~~), ~~taking into account that and~~ the intensification ~~and higher frequency~~ of
347 extreme events ~~result from is considered as~~ climate change (Barichivich et al., 2018).
348 Under these conditions, negative and positive fluxes of the two greenhouse gases were
349 found (negative values represented ~~ed~~ gas consumption). The negative CO₂ flux is
350 apparently a consequence of the increased CO₂ solubility in tidal waters or of the
351 increased sulfate reduction, as described in the literature (Borges et al., 2018;
352 Chowdhury et al., 2018; Nóbrega et al., 2016). Fluctuations in redox potential altered
353 the availability of the terminal electron acceptor and donor, and the forces of recovery
354 of their concentrations in the soil, such that a disproportionate release of CO₂ can result
355 from the alternative anaerobic degradation processes such as sulfate and iron reduction
356 (Chowdhury et al., 2018). The soil carbon flux in the mangrove area in the Amazon
357 region was within the range of findings for other tropical mangrove areas (2.6 to 11.0 g
358 CO₂ m⁻² d⁻¹; Shiao and Chiu, 2020). However, the mean flux of 6.2 mmol CO₂ m⁻² h⁻¹
359 recorded in this Amazonian mangrove was much higher than the mean efflux of 2.9
360 mmol CO₂ m⁻² h⁻¹ recorded in 75 mangroves during low tide periods (Alongi, 2009).

361 An emission of 0.01 Tg CH₄ y⁻¹, 0.6 g CH₄ m⁻² d⁻¹ (Rosentreter et al., 2018a), or 26.7
362 mg CH₄ m⁻² h⁻¹ has been reported for tropical latitudes (0 and 5°). In our study, the
363 monthly average of CH₄ flux was higher at the low (7.3 ± 8.0 mg CH₄ m⁻² h⁻¹) than at
364 the high topography (0.9 ± 0.6 mg C m⁻² h⁻¹), resulting in 0.1 g CH₄ m⁻² d⁻¹ or 0.5 Mg
365 CH₄ ha⁻¹ y⁻¹ (~~Figure-Fig.~~ 2). Therefore, the CH₄-C fluxes from the mangrove soil in the
366 Mojuim River estuary were much lower than expected. It is known that there is a
367 microbial functional module for CH₄ production and consumption (Xu et al., 2015) and
368 diffusibility of CH₄ (Sihi et al., 2018), and this module considers three key mechanisms:
369 acetoclastic methanogenesis (acetate production), hydrogenotrophic methanogenesis (H₂
370 and CO₂ production), and aerobic methanotrophy (CH₄ oxidation and O₂ reduction).
371 The average emission from the soil of 8.4 mmol CH₄ m⁻² d⁻¹ was well below the fluxes
372 recorded in the Bay of Bengal, with 18.4 mmol CH₄ m⁻² d⁻¹ (Biswas et al., 2007). In the
373 Amazonian mangrove studied the mean annual carbon equivalent efflux was 429.6 mg

374 | $\text{CO}_{2\text{-eq}} \text{ m}^{-2} \text{ h}^{-1}$. This value ~~is was insignificant~~ very low compared to the projected
375 | erosion losses of $103.5 \text{ Tg CO}_{2\text{-eq}} \text{ ha}^{-1} \text{ y}^{-1}$ for the next century in tropical mangrove
376 | forests (Adame et al., 2021). These higher CO_2 flux concomitantly with lower CH_4 flux
377 | in this Amazonian estuary are probably a consequence of changes in the rainfall pattern
378 | already underway, where the dry season was wetter and the rainy season drier when
379 | compared to the climatological normal. The most recent estimate between latitude 0° to
380 | 23.5° S shows an emission of $2.3 \text{ g CO}_2 \text{ m}^{-2} \text{ d}^{-1}$ (Rosentreter et al., 2018b). However,
381 | the efflux in the mangrove of the Mojuim River estuary was $6.7 \text{ g CO}_2 \text{ m}^{-2} \text{ d}^{-1}$. For the
382 | same latitudinal range, Rosentreter et al. (2018c) estimated an emission of $0.6 \text{ g CH}_4 \text{ m}^{-2}$
383 | d^{-1} , and we found an efflux of $0.1 \text{ g CH}_4 \text{ m}^{-2} \text{ d}^{-1}$.

384 | 4.2 Drivers of greenhouse gas fluxes

385 | Mangrove areas are periodically flooded, with a larger flood volume during the syzygy
386 | tides, especially in the rainy season. The hydrological condition of the soil is determined
387 | by the microtopography and can regulate the respiration of microorganisms (aerobic or
388 | anaerobic), being a decisive factor in controlling the CO_2 efflux (Dai et al., 2012;
389 | Davidson et al., 2000; Ehrenfeld, 1995). No significant influence on CO_2 flux was
390 | observed due to the low variation in high tide level throughout the year (0.19 m) (~~Figure~~
391 | ~~Fig. 2~~), although it was numerically higher at the high topography. However, tidal
392 | height and the rainy season resulted in a higher CO_2 flux (rate high/low =1.7) at the high
393 | topography ($7.86 \pm 0.04 \text{ g CO}_2 \text{ m}^{-2} \text{ d}^{-1}$) than at the low topography ($4.73 \pm 0.34 \text{ g CO}_2$
394 | $\text{m}^{-2} \text{ d}^{-1}$) (~~Figure-Fig. 2~~; SI 1). This result may be due to the root systems of most flood-
395 | tolerant plants remaining active when flooded (Angelov et al., 1996). Still, the high
396 | topography has longer flood-free periods, which only happens when the tides are
397 | syzygy or when the rains are torrential.

398 | CO_2 efflux was higher in the high topography than in the low topography in the rainy
399 | season (when soils are more subject to inundation), i.e., 39.8% lower in the forest soil
400 | exposed to the atmosphere for less time. Measurements performed on ~~62~~-mangrove
401 | forest soils showed an average flux of $2.87 \text{ mmol CO}_2 \text{ m}^{-2} \text{ h}^{-1}$ when the soil was
402 | exposed to the atmosphere (dry soil), while ~~75~~-results on flooded mangrove forest soils
403 | showed an average emission of $2.06 \text{ mmol CO}_2 \text{ m}^{-2} \text{ h}^{-1}$ (Alongi, 2007, 2009), i.e.,
404 | 28.2% less than for the dry soil. This reflects the increased facility gases have for
405 | molecular diffusion than fluids, and the increased surface area available for aerobic
406 | respiration and chemical oxidation during air exposure (Chen et al., 2010). Some studies

407 attribute this variation to the temperature of the soil when it is exposed to tropical air
408 (Alongi, 2009), which increases the export of dissolved inorganic carbon (Maher et al.,
409 2018). However, although despite the lack of significant variation in soil temperature
410 between topographies at each time of year (Figure-Fig. 4b), there was a positive
411 correlation (Pearson = 0.15, $p = 0.05$) between CO₂ efflux and soil temperature at the
412 low topography.

413 Some studies show that CH₄ efflux is a consequence of the seasonal temperature
414 variation in mangrove forest under temperate/monsoon climates (Chauhan et al., 2015;
415 Purvaja and Ramesh, 2001; Whalen, 2005). However, in your study CH₄ efflux was
416 correlated with Ta (Pearson = -0.33, $p < 0.00$) and RH (Pearson = 0.28, $p = 0.01$) only
417 in the dry season and at the low topography. The results show that the physical
418 parameters do not affect the fluxes in a standardized way, and their greater or lesser
419 influence depends on the topography and seasonality.

420 A compilation of several studies showed that the total CH₄ emissions from the soil in a
421 mangrove ecosystem range from 0 to 23.68 mg C m⁻² h⁻¹ (Shiau and Chiu, 2020), and
422 our study showed a range of -0.01 to 31.88 mg C m⁻² h⁻¹ (mean of 4.70 ± 5.00 mg C m⁻²
423 h⁻¹). The monthly CH₄ fluxes were generally higher at the low (0.232 ± 0.256 g CH₄ m⁻²
424 d⁻¹) than at the high (0.026 ± 0.018 g CH₄ m⁻² d⁻¹) topography, especially during the
425 rainy season when the tides were higher (Figure-Fig. 2). Only in the dry season was
426 there a significantly higher production at the low than at the high topography (Figure
427 Fig. 2; SI 1). The low topography produced 0.0249 g C m⁻² h⁻¹ more to the atmosphere
428 in the rainy season than in the dry season (Figure-Fig. 2), and a similar seasonal pattern
429 was recorded in other studies (Cameron et al., 2021).

430 The mangrove soil in the Mojuim River estuary is rich in silt and clay (Table 1), which
431 reduces sediment porosity and fosters the formation and maintenance of anoxic
432 conditions (Dutta et al., 2013). In addition, the lack of oxygen in the flooded mangrove
433 soil favors microbial processes such as denitrification, sulfate reduction,
434 methanogenesis, and redox reactions (Alongi and Christoffersen, 1992). A significant
435 amount of CH₄ produced in wetlands is dissolved in the pore water due to high pressure,
436 causing supersaturation, which allows CH₄ to be released by diffusion from the
437 sediment to the atmosphere and by boiling through the formation of bubbles.

438 Studies show that the CO₂ flux tends to be lower with high soil saturation (Chanda et
439 al., 2014; Kristensen et al., 2008). A total of 395 Mg C ha⁻¹ was found at the soil surface

440 (0.15 m) in the mangrove of the Mojuim River estuary, which was slightly higher than
441 the 340 Mg C ha⁻¹ found in other mangroves in the Amazon (Kauffman et al., 2018),
442 however being significantly 1.8 times greater at the low topography (Table 2). The finer
443 soil texture at the low topography (Table 1) reduces groundwater drainage which
444 facilitates the accumulation of C in the soil (Schmidt et al., 2011).

445 **4.3 Mangrove biomass**

446 Only the species *R. mangle* and *A. germinans* were found in the floristic survey carried
447 out, which is aligned with the results of other studies in the same region (Menezes et al.,
448 2008). Thus, the variations found in the flux between the topographies in the Mojuim
449 River estuary are not related to the mangrove forest structure, because there was no
450 difference in the aboveground biomass. Since there was no difference in the species
451 composition, the belowground biomass is not expected to differ either (Table 3).

452 Assuming that the amount of carbon stored is 42.0% of the total biomass (Sahu and
453 Kathiresan, 2019), the mangrove forest biomass of the Mojuim River estuary stores
454 127.9 and 138.9 Mg C ha⁻¹ at the high and low topographies, respectively. This result is
455 lower than the 507.8 Mg C ha⁻¹ estimated for Brazilian mangroves (Hamilton and
456 Friess, 2018), but are near the 103.7 Mg C ha⁻¹ estimated for a mangrove at Guará's
457 island (Salum et al., 2020), 108.4 Mg C ha⁻¹ for the Bragantina region (Gardunho,
458 2017), and 132.3 Mg C ha⁻¹ in French Guiana (Fromard et al., 1998). Thus, the biomass
459 found in the Mojuim estuary does not differ from the biomass found in other
460 Amazonian mangroves. The estimated primary production for tropical mangrove forests
461 is 218 ± 72 Tg C y⁻¹ (Bouillon et al., 2008).

462 **4.4 Biogeochemical parameters**

463 During the seasonal and annual periods, CH₄ efflux was not significantly correlated
464 with chemical parameters (Table 5), similar as observed in another study (Chen et al.,
465 2010). Flooded soils present reduced gas diffusion rates, which directly affects the
466 physiological state and activity of microbes, by limiting the supply of the dominant
467 electron acceptors (e.g., oxygen), and gases (e.g., CH₄) (Blagodatsky and Smith, 2012).
468 The importance of soil can be reflected in bacterial richness and diversity compared to
469 pore spaces filled with water (Banerjee et al., 2016). On the other hand, increasing soil
470 moisture provides the microorganisms with essential substrates such as ammonium,
471 nitrate, and soluble organic carbon, and increases gas diffusion rates in the water

472 (Blagodatsky and Smith, 2012). Biologically available nitrogen often limit marine
473 productivity (Bertics et al., 2010), and thus can affect CO₂ fluxes to the atmosphere.
474 However, a mangrove fertilization experiment showed that CH₄ emission rates were not
475 affected by N addition (Kreuzwieser et al., 2003). A higher concentration of C_{mic} and
476 N_{mic} in the dry period (Table 2), both in the high and low topographies, indicated that
477 microorganisms are more active when the soil spends more time aerated in the dry
478 period (Table 2), time when only the high tides produce anoxia in the mangrove soil
479 mainly in the low topography. Under reduced oxygen conditions, in a laboratory
480 incubated mangrove soil, the addition of nitrogen resulted in a significant increase in the
481 microbial metabolic quotient, showing no concomitant change in microbial respiration,
482 which was explained by a decrease in microbial biomass (Craig et al., 2021).

483 The high OM concentration at the two topographic locations (Table 2), at the two
484 seasons studied, and the respective negative correlation with CO₂ flux (Table 5) confirm
485 the importance of microbial activity in mangrove soils (Gao et al., 2020). Also, CH₄
486 produced in flooded soils can be converted mainly to CO₂ by the anaerobic oxidation of
487 CH₄ (Boetius et al., 2000; Milucka et al., 2015; Xu et al., 2015) which may contribute to
488 the higher CO₂ efflux in the Mojuim River estuary compared to other tropical
489 mangroves (Rosentreter et al., 2018b). The belowground C stock is considered the
490 largest C reservoir in a mangrove ecosystem, and it results from the low OM
491 decomposition rate due to flooding (Marchand, 2017).

492 The higher water salinity influenced by the tidal movement in the dry season (Table 1)
493 seems to result in a lower CH₄ flux at the low topography (Dutta et al., 2013; Lekphet et
494 al., 2005; Shiao and Chiu, 2020). High SO₄²⁻ concentration in the marine sediments
495 inhibits methane formation due to competition between SO₄²⁻ reduction and
496 methanogenic fermentation, as sulfate-reducing bacteria are more efficient at using
497 hydrogen than methanotrophic bacteria (Abram and Nedwell, 1978; Kristjansson et al.,
498 1982), a key factor fostering reduced CH₄ emissions. At high SO₄²⁻ concentrations
499 methanotrophic bacteria use CH₄ as an energy source and oxidize it to CO₂ (Coyne,
500 1999; Segarra et al., 2015), increasing the efflux of CO₂ and reduced CH₄ (Megonigal
501 and Schlesinger, 2002; Roslev and King, 1996). This may explain the high CO₂ and low
502 CH₄ efflux found throughout the year at the high and, especially, at the low
503 topographies (Figure Fig. 3).

504 Studies in coastal ecosystems in Taiwan have reported that methanotrophic bacteria can
505 be sensitive to soil pH, and reported an optimal growth at pH ranging from 6.5 to 7.5
506 (Shiau et al., 2018). The higher soil acidity in the Mojuim River wetland (Table 1) may
507 be inhibiting the activity of methanogenic bacteria by increasing the population of
508 methanotrophic bacteria, which are efficient in CH₄ consumption (Chen et al., 2010;
509 Hegde et al., 2003; Shiau and Chiu, 2020). In addition, the pneumatophores present in
510 *R. mangle* increase soil aeration and reduce CH₄ emissions (Allen et al., 2011; He et al.,
511 2019). Spatial differences (topography) in CH₄ emissions in the soil can be attributed to
512 substrate heterogeneity, salinity, and the abundance of methanogenic and
513 methanotrophic bacteria (Gao et al., 2020). Increases in CH₄ efflux with reduced
514 salinity were found as a consequence of intense oxidation or reduced competition from
515 the more energetically efficient SO₄²⁻ and NO₃³⁻ reducing bacteria when compared to the
516 methanogenic bacteria (Biswas et al., 2007). This fact can be observed in the CH₄ efflux
517 in the mangrove of the Mojuim River, because there was an increased CH₄ production
518 | especially in the low topography in the rainy season (Figure-Fig. 3), when water salinity
519 | is reduced (Table 1) due to the increased precipitation. However, we did not find a
520 | correlation between CH₄ efflux and salinity, as previously reported (Purvaja and
521 | Ramesh, 2001).

522 5 Conclusions

523 Seasonality was important for CH₄ efflux but did not influence CO₂ efflux. The
524 differences in fluxes may be an effect of global climate changes on the terrestrial
525 biogeochemistry at the plant-soil-atmosphere interface, as indicated by the deviation in
526 precipitation values from the climatology normal, making it necessary to extend this
527 study for more years. Using the factor of 23 to convert the global warming potential of
528 CH₄ to CO₂ (IPCC, 2001), the CO₂ equivalent emission was 35.4 Mg CO_{2-eq} ha⁻¹ yr⁻¹.
529 Over a 100-year time period, a radiative forcing due to the continuous emission of 0.05
530 kg CH₄ m⁻² y⁻¹ found in this study, would be offset if CO₂ sequestration rates were 2.16
531 kg CO₂ m⁻² y⁻¹ (Neubauer and Megonigal, 2015).

532 Microtopography should be considered when determining the efflux of CO₂ and CH₄ in
533 mangrove forests in an Amazon estuary. The low topography in the mangrove forest of
534 Mojuim River had a higher concentration of organic carbon in the soil. However, it did
535 not produce a higher CO₂ efflux because it was negatively influenced by soil moisture,
536 | which was indifferent to CH₄ efflux. ~~MOQM~~, C/N ratio, and Eh were critical in soil

537 microbial activity, which resulted in a variation in CO₂ flux during the year and
538 seasonal periods. Thus, the physicochemical properties of the soil are important for CO₂
539 flux, especially in the rainy season. Still, they did not influence CH₄ fluxes.

540 *Data availability:* The data used in this article belong to the doctoral thesis of Saul
541 Castellón, within the Postgraduate Program in Environmental Sciences, at the Federal
542 University of Pará. Access to the data can be requested from Dr. Castellón
543 (saulmarz22@gmail.com), which holds the set of all data used in this paper.

544 *Author contributions:* SEMC and JHC designed the study and wrote the article with the
545 help of JFB, MR, MLR, and CN. JFB assisted in the field experiment. MR provided
546 logistical support in field activities.

547 *Competing interests:* The authors declare that they have no conflict of interest

548 *Acknowledgements:* The authors are grateful to the Program of Alliances for Education
549 and Training of the Organization of the American States and to Coimbra Group of
550 Brazilian Universities, for the financial support, as well as to Paulo Sarmento for the
551 assistance at laboratory analysis, and to Maridalva Ribeiro and Lucivaldo da Silva for
552 the fieldwork assistance. Furthermore, the authors would like to thank the Laboratory of
553 Biogeochemical Cycles (Geosciences Institute, Federal University of Pará) for the
554 equipment provided for this research.

555 **6 References**

556 Abram, J. W. and Nedwell, D. B.: Inhibition of methanogenesis by sulphate reducing
557 bacteria competing for transferred hydrogen, *Arch. Microbiol.*, 117(1), 89–92,
558 doi:10.1007/BF00689356, 1978.

559 Adame, M. F., Connolly, R. M., Turschwell, M. P., Lovelock, C. E., Fatoyinbo, T.,
560 Lagomasino, D., Goldberg, L. A., Holdorf, J., Friess, D. A., Sasmito, S. D., Sanderman,
561 J., Sievers, M., Buelow, C., Kauffman, J. B., Bryan-Brown, D. and Brown, C. J.: Future
562 carbon emissions from global mangrove forest loss, *Glob. Chang. Biol.*, 27(12), 2856–
563 2866, doi:10.1111/gcb.15571, 2021.

564 Allen, D., Dalal, R. C., Rennenberg, H. and Schmidt, S.: Seasonal variation in nitrous
565 oxide and methane emissions from subtropical estuary and coastal mangrove sediments,
566 *Australia, Plant Biol.*, 13(1), 126–133, doi:10.1111/j.1438-8677.2010.00331.x, 2011.

567 Almeida, R. F. de, Mikhael, J. E. R., Franco, F. O., Santana, L. M. F. and Wendling, B.:

568 Measuring the labile and recalcitrant pools of carbon and nitrogen in forested and
569 agricultural soils: A study under tropical conditions, *Forests*, 10(7), 544,
570 doi:10.3390/f10070544, 2019.

571 Alongi, D. M.: The contribution of mangrove ecosystems to global carbon cycling and
572 greenhouse gas emissions, in *Greenhouse gas and carbon balances in mangrove coastal*
573 *ecosystems*, edited by Y. Tateda, R. Upstill-Goddard, T. Goreau, D. M. Alongi, A.
574 Nose, E. Kristensen, and G. Wattayakorn, pp. 1–10, Gendai Tosho, Kanagawa, Japan.,
575 2007.

576 Alongi, D. M.: *The Energetics of Mangrove Forests*, Springer Netherlands, Dordrecht.,
577 2009.

578 Alongi, D. M. and Christoffersen, P.: Benthic infauna and organism-sediment relations
579 in a shallow, tropical coastal area: influence of outwelled mangrove detritus and
580 physical disturbance, *Mar. Ecol. Prog. Ser.*, 81(3), 229–245, doi:10.3354/meps081229,
581 1992.

582 Alongi, D. M. and Mukhopadhyay, S. K.: Contribution of mangroves to coastal carbon
583 cycling in low latitude seas, *Agric. For. Meteorol.*, 213, 266–272,
584 doi:10.1016/j.agrformet.2014.10.005, 2015.

585 Angelov, M. N., Sung, S. J. S., Doong, R. Lou, Harms, W. R., Kormanik, P. P. and
586 Black, C. C.: Long-and short-term flooding effects on survival and sink-source
587 relationships of swamp-adapted tree species, *Tree Physiol.*, 16(4), 477–484,
588 doi:10.1093/treephys/16.5.477, 1996.

589 Araujo, A. S. F. de: Is the microwave irradiation a suitable method for measuring soil
590 microbial biomass?, *Rev. Environ. Sci. Biotechnol.*, 9(4), 317–321,
591 doi:10.1007/s11157-010-9210-y, 2010.

592 Banerjee, S., Helgason, B., Wang, L., Winsley, T., Ferrari, B. C. and Siciliano, S. D.:
593 Legacy effects of soil moisture on microbial community structure and N₂O emissions,
594 *Soil Biol. Biochem.*, 95, 40–50, doi:10.1016/j.soilbio.2015.12.004, 2016.

595 Barichivich, J., Gloor, E., Peylin, P., Brienen, R. J. W., Schöngart, J., Espinoza, J. C.
596 and Pattanayak, K. C.: Recent intensification of Amazon flooding extremes driven by
597 strengthened Walker circulation, *Sci. Adv.*, 4(9), doi:10.1126/sciadv.aat8785, 2018.

598 Bastviken, D., Tranvik, L. J., Downing, J. A., Crill, P. M. and Enrich-Prast, A.:

599 Freshwater Methane Emissions Offset the Continental Carbon Sink, *Science* (80-.),
600 331(6013), 50–50, doi:10.1126/science.1196808, 2011.

601 Bauza, J. F., Morell, J. M. and Corredor, J. E.: Biogeochemistry of Nitrous Oxide
602 Production in the Red Mangrove (*Rhizophora mangle*) Forest Sediments, *Estuar. Coast.*
603 *Shelf Sci.*, 55(5), 697–704, doi:10.1006/ECSS.2001.0913, 2002.

604 Bertics, V. J., Sohm, J. A., Treude, T., Chow, C. E. T., Capone, D. G., Fuhrman, J. A.
605 and Ziebis, W.: Burrowing deeper into benthic nitrogen cycling: The impact of
606 Bioturbation on nitrogen fixation coupled to sulfate reduction, *Mar. Ecol. Prog. Ser.*,
607 409, 1–15, doi:10.3354/meps08639, 2010.

608 Biswas, H., Mukhopadhyay, S. K., Sen, S. and Jana, T. K.: Spatial and temporal
609 patterns of methane dynamics in the tropical mangrove dominated estuary, NE coast of
610 Bay of Bengal, India, *J. Mar. Syst.*, 68(1–2), 55–64, doi:10.1016/j.jmarsys.2006.11.001,
611 2007.

612 Blagodatsky, S. and Smith, P.: Soil physics meets soil biology: Towards better
613 mechanistic prediction of greenhouse gas emissions from soil, *Soil Biol. Biochem.*, 47,
614 78–92, doi:10.1016/J.SOILBIO.2011.12.015, 2012.

615 Boetius, A., Ravensschlag, K., Schubert, C. J., Rickert, D., Widdel, F., Gleseke, A.,
616 Amann, R., Jørgensen, B. B., Witte, U. and Pfannkuche, O.: A marine microbial
617 consortium apparently mediating anaerobic oxidation methane, *Nature*, 407(6804), 623–
618 626, doi:10.1038/35036572, 2000.

619 Borges, A. V., Abril, G., Darchambeau, F., Teodoru, C. R., Deborde, J., Vidal, L. O.,
620 Lambert, T. and Bouillon, S.: Divergent biophysical controls of aquatic CO₂ and CH₄
621 in the World's two largest rivers, *Sci. Rep.*, 5, doi:10.1038/srep15614, 2015.

622 Borges, A. V., Abril, G. and Bouillon, S.: Carbon dynamics and CO₂ and CH₄
623 outgassing in the Mekong delta, *Biogeosciences*, 15(4), 1093–1114, doi:10.5194/bg-15-
624 1093-2018, 2018.

625 Bouillon, S., Borges, A. V., Castañeda-Moya, E., Diele, K., Dittmar, T., Duke, N. C.,
626 Kristensen, E., Lee, S. Y., Marchand, C., Middelburg, J. J., Rivera-Monroy, V. H.,
627 Smith, T. J. and Twilley, R. R.: Mangrove production and carbon sinks: A revision of
628 global budget estimates, *Global Biogeochem. Cycles*, 22(2), 1–12,
629 doi:10.1029/2007GB003052, 2008.

630 Brookes, P. C., Landman, A., Pruden, G. and Jenkinson, D. S.: Chloroform fumigation
631 and the release of soil nitrogen: A rapid direct extraction method to measure microbial
632 biomass nitrogen in soil, *Soil Biol. Biochem.*, 17(6), 837–842, doi:10.1016/0038-
633 0717(85)90144-0, 1985.

634 Cameron, C., Hutley, L. B., Munksgaard, N. C., Phan, S., Aung, T., Thinn, T., Aye, W.
635 M. and Lovelock, C. E.: Impact of an extreme monsoon on CO₂ and CH₄ fluxes from
636 mangrove soils of the Ayeyarwady Delta, Myanmar, *Sci. Total Environ.*, 760, 143422,
637 doi:10.1016/j.scitotenv.2020.143422, 2021.

638 Castillo, J. A. A., Apan, A. A., Maraseni, T. N. and Salmo, S. G.: Soil greenhouse gas
639 fluxes in tropical mangrove forests and in land uses on deforested mangrove lands,
640 *Catena*, 159, 60–69, doi:10.1016/j.catena.2017.08.005, 2017.

641 Chanda, A., Akhand, A., Manna, S., Dutta, S., Das, I., Hazra, S., Rao, K. H. and
642 Dadhwal, V. K.: Measuring daytime CO₂ fluxes from the inter-tidal mangrove soils of
643 Indian Sundarbans, *Environ. Earth Sci.*, 72(2), 417–427, doi:10.1007/s12665-013-2962-
644 2, 2014.

645 Chauhan, R., Datta, A., Ramanathan, A. and Adhya, T. K.: Factors influencing spatio-
646 temporal variation of methane and nitrous oxide emission from a tropical mangrove of
647 eastern coast of India, *Atmos. Environ.*, 107, 95–106,
648 doi:10.1016/j.atmosenv.2015.02.006, 2015.

649 Chen, G. C., Tam, N. F. Y. and Ye, Y.: Spatial and seasonal variations of atmospheric
650 N₂O and CO₂ fluxes from a subtropical mangrove swamp and their relationships with
651 soil characteristics, *Soil Biol. Biochem.*, 48, 175–181,
652 doi:10.1016/j.soilbio.2012.01.029, 2012.

653 Chen, G. C., Ulumuddin, Y. I., Pramudji, S., Chen, S. Y., Chen, B., Ye, Y., Ou, D. Y.,
654 Ma, Z. Y., Huang, H. and Wang, J. K.: Rich soil carbon and nitrogen but low
655 atmospheric greenhouse gas fluxes from North Sulawesi mangrove swamps in
656 Indonesia, *Sci. Total Environ.*, 487(1), 91–96, doi:10.1016/j.scitotenv.2014.03.140,
657 2014.

658 Chen, G. C. C., Tam, N. F. Y. F. Y. and Ye, Y.: Summer fluxes of atmospheric
659 greenhouse gases N₂O, CH₄ and CO₂ from mangrove soil in South China, *Sci. Total
660 Environ.*, 408(13), 2761–2767, doi:10.1016/j.scitotenv.2010.03.007, 2010.

661 Chowdhury, T. R., Bramer, L., Hoyt, D. W., Kim, Y. M., Metz, T. O., McCue, L. A.,
662 Diefenderfer, H. L., Jansson, J. K. and Bailey, V.: Temporal dynamics of CO₂ and CH₄
663 loss potentials in response to rapid hydrological shifts in tidal freshwater wetland soils,
664 *Ecol. Eng.*, 114, 104–114, doi:10.1016/j.ecoleng.2017.06.041, 2018.

665 Chuang, P. C., Young, M. B., Dale, A. W., Miller, L. G., Herrera-Silveira, J. A. and
666 Paytan, A.: Methane and sulfate dynamics in sediments from mangrove-dominated
667 tropical coastal lagoons, Yucatan, Mexico, *Biogeosciences*, 13(10), 2981–3001, 2016.

668 Coyne, M.: *Soil Microbiology: An Exploratory Approach*, Delmar Publishers, New
669 York, NY, USA., 1999.

670 Craig, H., Antwis, R. E., Cordero, I., Ashworth, D., Robinson, C. H., Osborne, T. Z.,
671 Bardgett, R. D., Rowntree, J. K. and Simpson, L. T.: Nitrogen addition alters
672 composition, diversity, and functioning of microbial communities in mangrove soils:
673 An incubation experiment, *Soil Biol. Biochem.*, 153, 108076,
674 doi:10.1016/j.soilbio.2020.108076, 2021.

675 Dai, Z., Trettin, C. C., Li, C., Li, H., Sun, G. and Amatya, D. M.: Effect of Assessment
676 Scale on Spatial and Temporal Variations in CH₄, CO₂, and N₂O Fluxes in a Forested
677 Wetland, *Water, Air, Soil Pollut.*, 223(1), 253–265, doi:10.1007/s11270-011-0855-0,
678 2012.

679 Davidson, E. A., Verchot, L. V., Cattanio, J. H., Ackerman, I. L. and Carvalho, J. E. M.:
680 Effects of soil water content on soil respiration in forests and cattle pastures of eastern
681 Amazonia, *Biogeochemistry*, 48(1), 53–69, doi:10.1023/a:1006204113917, 2000.

682 Donato, D. C., Kauffman, J. B., Murdiyarso, D., Kurnianto, S., Stidham, M. and
683 Kanninen, M.: Mangroves among the most carbon-rich forests in the tropics, *Nat.*
684 *Geosci.*, 4(5), 293–297, doi:10.1038/ngeo1123, 2011.

685 Dutta, M. K., Chowdhury, C., Jana, T. K. and Mukhopadhyay, S. K.: Dynamics and
686 exchange fluxes of methane in the estuarine mangrove environment of the Sundarbans,
687 NE coast of India, *Atmos. Environ.*, 77, 631–639, doi:10.1016/j.atmosenv.2013.05.050,
688 2013.

689 Ehrenfeld, J. G.: Microsite differences in surface substrate characteristics in
690 *Chamaecyparis* swamps of the New Jersey Pinelands, *Wetlands*, 15(2), 183–189,
691 doi:10.1007/BF03160672, 1995.

692 El-Robrini, M., Alves, M. A. M. S., Souza Filho, P. W. M., El-Robrini M. H. S., Silva
693 Júnior, O. G. and França, C. F.: Atlas de Erosão e Progradação da zona costeira do
694 Estado do Pará – Região Amazônica: Áreas oceânica e estuarina, in Atlas de Erosão e
695 Progradação da Zona Costeira Brasileira, edited by D. Muehe, pp. 1–34, São Paulo.,
696 2006.

697 EPA, E. P. A.: Inventory of U.S. Greenhouse Gas Emissions and Sinks: 1990–2015.,
698 2017.

699 Fernandes, W. A. A. and Pimentel, M. A. da S.: Dinâmica da paisagem no entorno da
700 RESEX marinha de São João da Ponta/PA: utilização de métricas e geoprocessamento,
701 Caminhos Geogr., 20(72), 326–344, doi:10.14393/RCG207247140, 2019.

702 Ferreira, A. S., Camargo, F. A. O. and Vidor, C.: Utilização de microondas na avaliação
703 da biomassa microbiana do solo, Rev. Bras. Ciência do Solo, 23(4), 991–996,
704 doi:10.1590/S0100-06831999000400026, 1999.

705 Ferreira, S. da S.: Entre marés e mangues: paisagens territorializadas por pescadores da
706 resex marinha de São João da Ponta (PA), Federal University of Pará., 2017.

707 França, C. F. de, Pimentel, M. A. D. S. and Neves, S. C. R.: Estrutura Paisagística De
708 São João Da Ponta, Nordeste Do Pará, Geogr. Ensino Pesqui., 20(1), 130–142,
709 doi:10.5902/2236499418331, 2016.

710 Frankignoulle, M.: Field measurements of air-sea CO₂ exchange, Limnol. Oceanogr.,
711 33(3), 313–322, 1988.

712 Friesen, S. D., Dunn, C. and Freeman, C.: Decomposition as a regulator of carbon
713 accretion in mangroves: a review, Ecol. Eng., 114, 173–178,
714 doi:10.1016/j.ecoleng.2017.06.069, 2018.

715 Fromard, F., Puig, H., Cadamuro, L., Marty, G., Betoulle, J. L. and Mougin, E.:
716 Structure, above-ground biomass and dynamics of mangrove ecosystems: new data
717 from French Guiana, Oecologia, 115(1), 39–53, doi:10.1007/s004420050489, 1998.

718 Gao, G. F., Zhang, X. M., Li, P. F., Simon, M., Shen, Z. J., Chen, J., Gao, C. H. and
719 Zheng, H. L.: Examining Soil Carbon Gas (CO₂, CH₄) Emissions and the Effect on
720 Functional Microbial Abundances in the Zhangjiang Estuary Mangrove Reserve, J.
721 Coast. Res., 36(1), 54–62, doi:10.2112/JCOASTRES-D-18-00107.1, 2020.

722 Gardunho, D. C. L.: Estimativas de biomassa acima do solo da floresta de mangue na

723 península de Ajuruteua, Bragança – PA, Federal University of Pará, Belém, Brazil.,
724 2017.

725 Hamilton, S. E. and Friess, D. A.: Global carbon stocks and potential emissions due to
726 mangrove deforestation from 2000 to 2012, *Nat. Clim. Chang.*, 8(3), 240–244,
727 doi:10.1038/s41558-018-0090-4, 2018.

728 He, Y., Guan, W., Xue, D., Liu, L., Peng, C., Liao, B., Hu, J., Zhu, Q., Yang, Y., Wang,
729 X., Zhou, G., Wu, Z. and Chen, H.: Comparison of methane emissions among invasive
730 and native mangrove species in Dongzhaigang, Hainan Island, *Sci. Total Environ.*, 697,
731 133945, doi:10.1016/j.scitotenv.2019.133945, 2019.

732 Hegde, U., Chang, T.-C. and Yang, S.-S.: Methane and carbon dioxide emissions from
733 Shan-Chu-Ku landfill site in northern Taiwan., *Chemosphere*, 52(8), 1275–1285,
734 doi:10.1016/S0045-6535(03)00352-7, 2003.

735 Herz, R.: *Manguezais do Brasil*, Instituto Oceanografico da USP/CIRM, São Paulo,
736 Brazil., 1991.

737 Howard, J., Hoyt, S., Isensee, K., Telszewski, M. and Pidgeon, E.: *Coastal Blue*
738 *Carbon: Methods for Assessing Carbon Stocks and Emissions Factors in Mangroves,*
739 *Tidal Salt Marshes, and Seagrasses*, edited by J. Howard, S. Hoyt, K. Isensee, M.
740 Telszewski, and E. Pidgeon, International Union for Conservation of Nature, Arlington,
741 Virginia, USA. [online] Available from:
742 http://www.cifor.org/publications/pdf_files/Books/BMurdiyarso1401.pdf (Accessed 11
743 September 2019), 2014.

744 IPCC: *Climate Change 2001: Third Assessment Report of the IPCC*, Cambridge., 2001.

745 Islam, K. R. and Weil, R. R.: Microwave irradiation of soil for routine measurement of
746 microbial biomass carbon, *Biol. Fertil. Soils*, 27(4), 408–416,
747 doi:10.1007/s003740050451, 1998.

748 Kalembara, S. J. and Jenkinson, D. S.: A comparative study of titrimetric and
749 gravimetric methods for determination of organic carbon in soil, *J. Sci. Food Agric.*, 24,
750 1085–1090, 1973.

751 Kauffman, B. J., Donato, D. and Adame, M. F.: *Protocolo para la medición, monitoreo*
752 *y reporte de la estructura, biomasa y reservas de carbono de los manglares*, Bogor,
753 Indonesia., 2013.

754 Kauffman, J. B., Bernardino, A. F., Ferreira, T. O., Giovannoni, L. R., de O. Gomes, L.
755 E., Romero, D. J., Jimenez, L. C. Z. and Ruiz, F.: Carbon stocks of mangroves and salt
756 marshes of the Amazon region, Brazil, *Biol. Lett.*, 14(9), 20180208,
757 doi:10.1098/rsbl.2018.0208, 2018.

758 Kreuzwieser, J., Buchholz, J. and Rennenberg, H.: Emission of Methane and Nitrous
759 Oxide by Australian Mangrove Ecosystems, *Plant Biol.*, 5(4), 423–431, doi:10.1055/s-
760 2003-42712, 2003.

761 Kristensen, E., Bouillon, S., Dittmar, T. and Marchand, C.: Organic carbon dynamics in
762 mangrove ecosystems: A review, *Aquat. Bot.*, 89(2), 201–219,
763 doi:10.1016/J.AQUABOT.2007.12.005, 2008.

764 Kristjansson, J. K., Schönheit, P. and Thauer, R. K.: Different K_s values for hydrogen
765 of methanogenic bacteria and sulfate reducing bacteria: An explanation for the apparent
766 inhibition of methanogenesis by sulfate, *Arch. Microbiol.*, 131(3), 278–282,
767 doi:10.1007/BF00405893, 1982.

768 Lekphet, S., Nitorisavut, S. and Adsavakulchai, S.: Estimating methane emissions from
769 mangrove area in Ranong Province, Thailand, *Songklanakarin J. Sci. Technol.*, 27(1),
770 153–163 [online] Available from: <https://www.researchgate.net/publication/26473398>
771 (Accessed 29 January 2019), 2005.

772 Maher, D. T., Call, M., Santos, I. R. and Sanders, C. J.: Beyond burial: Lateral
773 exchange is a significant atmospheric carbon sink in mangrove forests, *Biol. Lett.*,
774 14(7), 1–4, doi:10.1098/rsbl.2018.0200, 2018.

775 Mahesh, P., Sreenivas, G., Rao, P. V. N. N., Dadhwal, V. K., Sai Krishna, S. V. S. S.
776 and Mallikarjun, K.: High-precision surface-level CO₂ and CH₄ using off-axis
777 integrated cavity output spectroscopy (OA-ICOS) over Shadnagar, India, *Int. J. Remote*
778 *Sens.*, 36(22), 5754–5765, doi:10.1080/01431161.2015.1104744, 2015.

779 Marchand, C.: Soil carbon stocks and burial rates along a mangrove forest
780 chronosequence (French Guiana), *For. Ecol. Manage.*, 384, 92–99,
781 doi:10.1016/j.foreco.2016.10.030, 2017.

782 McEwing, K. R., Fisher, J. P. and Zona, D.: Environmental and vegetation controls on
783 the spatial variability of CH₄ emission from wet-sedge and tussock tundra ecosystems
784 in the Arctic, *Plant Soil*, 388(1–2), 37–52, doi:10.1007/s11104-014-2377-1, 2015.

785 Megonigal, J. P. and Schlesinger, W. H.: Methane-limited methanotrophy in tidal
786 freshwater swamps, *Global Biogeochem. Cycles*, 16(4), 35-1-35-10,
787 doi:10.1029/2001GB001594, 2002.

788 Menezes, M. P. M. de, Berger, U. and Mehlig, U.: Mangrove vegetation in Amazonia :
789 a review of studies from the coast of Pará and Maranhão States , north Brazil, *Acta*
790 *Amaz.*, 38(3), 403-420, doi:10.1590/S0044-59672008000300004, 2008.

791 Milucka, J., Kirf, M., Lu, L., Krupke, A., Lam, P., Littmann, S., Kuypers, M. M. M. and
792 Schubert, C. J.: Methane oxidation coupled to oxygenic photosynthesis in anoxic
793 waters, *ISME J.*, 9(9), 1991-2002, doi:10.1038/ismej.2015.12, 2015.

794 Monz, C. A., Reuss, D. E. and Elliott, E. T.: Soil microbial biomass carbon and nitrogen
795 estimates using 2450 MHz microwave irradiation or chloroform fumigation followed by
796 direct extraction, *Agric. Ecosyst. Environ.*, 34(1-4), 55-63, doi:10.1016/0167-
797 8809(91)90093-D, 1991.

798 Neubauer, S. C. and Megonigal, J. P.: Moving Beyond Global Warming Potentials to
799 Quantify the Climatic Role of Ecosystems, *Ecosystems*, 18(6), 1000-1013,
800 doi:10.1007/S10021-015-9879-4/TABLES/2, 2015.

801 Nóbrega, G. N., Ferreira, T. O., Siqueira Neto, M., Queiroz, H. M., Artur, A. G.,
802 Mendonça, E. D. S., Silva, E. D. O. and Otero, X. L.: Edaphic factors controlling
803 summer (rainy season) greenhouse gas emissions (CO₂ and CH₄) from semiarid
804 mangrove soils (NE-Brazil), *Sci. Total Environ.*, 542, 685-693,
805 doi:10.1016/j.scitotenv.2015.10.108, 2016.

806 Norman, J. M., Kucharik, C. J., Gower, S. T., Baldocchi, D. D., Crill, P. M., Rayment,
807 M., Savage, K. and Striegl, R. G.: A comparison of six methods for measuring soil-
808 surface carbon dioxide fluxes, *J. Geophys. Res. Atmos.*, 102(D24), 28771-28777,
809 doi:10.1029/97JD01440, 1997.

810 Peel, M. C., Finlayson, B. L. and McMahon, T. A.: Updated world map of the Köppen-
811 Geiger climate classification, *Hydrol. Earth Syst. Sci.*, 11(5), 1633-1644,
812 doi:10.1002/ppp.421, 2007.

813 Poffenbarger, H. J., Needelman, B. A. and Megonigal, J. P.: Salinity Influence on
814 Methane Emissions from Tidal Marshes, *Wetlands*, 31(5), 831-842,
815 doi:10.1007/s13157-011-0197-0, 2011.

816 Prost, M. T., Mendes, A. C., Faure, J. F., Berredo, J. F., Sales, M. E. ., Furtado, L. G.,
817 Santana, M. G., Silva, C. A., Nascimento, I. ., Gorayeb, I., Secco, M. F. and Luz, L.:
818 Manguezais e estuários da costa paraense: exemplo de estudo multidisciplinar integrado
819 (Marapanim e São Caetano de Odivelas), in *Ecosystemas Costeiros: Impactos e Gestão*
820 *Ambiental*, edited by M. T. Prost and A. Mendes, pp. 25–52, FUNTEC and Paraense
821 Museum “Emílio Goeldi,” Belém, Brazil., 2001.

822 Purvaja, R. and Ramesh, R.: Natural and Anthropogenic Methane Emission from
823 Coastal Wetlands of South India, *Environ. Manage.*, 27(4), 547–557,
824 doi:10.1007/s002670010169, 2001.

825 Purvaja, R., Ramesh, R. and Frenzel, P.: Plant-mediated methane emission from an
826 Indian mangrove, *Glob. Chang. Biol.*, 10(11), 1825–1834, doi:10.1111/j.1365-
827 2486.2004.00834.x, 2004.

828 Reeburgh, W. S.: Oceanic Methane Biogeochemistry, *Chem. Rev.*, 2, 486–513,
829 doi:10.1021/cr050362v, 2007.

830 Robertson, A. I., Alongi, D. M. and Boto, K. G.: Food chains and carbon fluxes, in
831 *Coastal and Estuarine Studies*, edited by A. I. Robertson and D. M. Alongi, pp. 293–
832 326, American Geophysical Union., 1992.

833 Rocha, A. S.: Caracterização física do estuário do rio Mojuim em São Caetano de
834 Odivelas - PA, Federal University of Pará. [online] Available from:
835 <http://repositorio.ufpa.br/jspui/handle/2011/11390>, 2015.

836 Rollnic, M., Costa, M. S., Medeiros, P. R. L. and Monteiro, S. M.: Tide Influence on
837 Suspended Matter Transport in an Amazonian Estuary, *J. Coast. Res.*, 85, 121–125,
838 doi:10.2112/SI85-025.1, 2018.

839 Rosentreter, J. A., Maher, D. T., Erler, D. V., Murray, R. H. and Eyre, B. D.: Methane
840 emissions partially offset “blue carbon” burial in mangroves, *Sci. Adv.*, 4(6), 1–11,
841 doi:10.1126/sciadv.aao4985, 2018a.

842 Rosentreter, J. A., Maher, D. . T., Erler, D. V. V., Murray, R. and Eyre, B. D. D.:
843 Seasonal and temporal CO₂ dynamics in three tropical mangrove creeks – A revision of
844 global mangrove CO₂ emissions, *Geochim. Cosmochim. Acta*, 222, 729–745,
845 doi:10.1016/j.gca.2017.11.026, 2018b.

846 Roslev, P. and King, G. M.: Regulation of methane oxidation in a freshwater wetland by

847 water table changes and anoxia, *FEMS Microbiol. Ecol.*, 19(2), 105–115,
848 doi:10.1111/j.1574-6941.1996.tb00203.x, 1996.

849 Sahu, S. K. and Kathiresan, K.: The age and species composition of mangrove forest
850 directly influence the net primary productivity and carbon sequestration potential,
851 *Biocatal. Agric. Biotechnol.*, 20, 101235, doi:10.1016/j.bcab.2019.101235, 2019.

852 Salum, R. B., Souza-Filho, P. W. M., Simard, M., Silva, C. A., Fernandes, M. E. B.,
853 Cougo, M. F., do Nascimento, W. and Rogers, K.: Improving mangrove above-ground
854 biomass estimates using LiDAR, *Estuar. Coast. Shelf Sci.*, 236, 106585,
855 doi:10.1016/j.ecss.2020.106585, 2020.

856 Schmidt, M. W. I., Torn, M. S., Abiven, S., Dittmar, T., Guggenberger, G., Janssens, I.
857 A., Kleber, M., Kögel-Knabner, I., Lehmann, J., Manning, D. A. C., Nannipieri, P.,
858 Rasse, D. P., Weiner, S. and Trumbore, S. E.: Persistence of soil organic matter as an
859 ecosystem property, *Nature*, 478(7367), 49–56, doi:10.1038/nature10386, 2011.

860 Segarra, K. E. A., Schubotz, F., Samarkin, V., Yoshinaga, M. Y., Hinrichs, K. U. and
861 Joye, S. B.: High rates of anaerobic methane oxidation in freshwater wetlands reduce
862 potential atmospheric methane emissions, *Nat. Commun.*, 6(1), 1–8,
863 doi:10.1038/ncomms8477, 2015.

864 Shiau, Y.-J. and Chiu, C.-Y.: Biogeochemical Processes of C and N in the Soil of
865 Mangrove Forest Ecosystems, *Forests*, 11(5), 492, doi:10.3390/f11050492, 2020.

866 Shiau, Y. J., Cai, Y., Lin, Y. Te, Jia, Z. and Chiu, C. Y.: Community Structure of Active
867 Aerobic Methanotrophs in Red Mangrove (*Kandelia obovata*) Soils Under Different
868 Frequency of Tides, *Microb. Ecol.*, 75(3), 761–770, doi:10.1007/s00248-017-1080-1,
869 2018.

870 Sihi, D., Davidson, E. A., Chen, M., Savage, K. E., Richardson, A. D., Keenan, T. F.
871 and Hollinger, D. Y.: Merging a mechanistic enzymatic model of soil heterotrophic
872 respiration into an ecosystem model in two AmeriFlux sites of northeastern USA,
873 *Agric. For. Meteorol.*, 252, 155–166, doi:10.1016/J.AGRFORMET.2018.01.026, 2018.

874 Souza Filho, P. W. M.: Costa de manguezais de macromaré da Amazônia: cenários
875 morfológicos, mapeamento e quantificação de áreas usando dados de sensores remotos,
876 *Rev. Bras. Geofísica*, 23(4), 427–435, doi:10.1590/S0102-261X2005000400006, 2005.

877 Sparling, G. P. and West, A. W.: A direct extraction method to estimate soil microbial

878 C: calibration in situ using microbial respiration and ¹⁴C labelled cells, *Soil Biol.*
879 *Biochem.*, 20(3), 337–343, doi:10.1016/0038-0717(88)90014-4, 1988.

880 Sundqvist, E., Vestin, P., Crill, P., Persson, T. and Lindroth, A.: Short-term effects of
881 thinning, clear-cutting and stump harvesting on methane exchange in a boreal forest,
882 *Biogeosciences*, 11(21), 6095–6105, doi:10.5194/bg-11-6095-2014, 2014.

883 Valentim, M., Monteiro, S. and Rollnic, M.: The Influence of Seasonality on Haline
884 Zones in An Amazonian Estuary, *J. Coast. Res.*, 85, 76–80, doi:10.2112/SI85-016.1,
885 2018.

886 Valentine, D. L.: Emerging Topics in Marine Methane Biogeochemistry, *Ann. Rev.*
887 *Mar. Sci.*, 3(1), 147–171, doi:10.1146/annurev-marine-120709-142734, 2011.

888 Vance, E. D., Brookes, P. C. and Jenkinson, D. S.: An extraction method for measuring
889 soil microbial biomass C, *Soil Biol. Biochem.*, 19(6), 703–707, doi:10.1016/0038-
890 0717(87)90052-6, 1987.

891 Verchot, L. V., Davidson, E. A., Cattânio, J. H. and Ackerman, I. L.: Land-use change
892 and biogeochemical controls of methane fluxes in soils of eastern Amazonia,
893 *Ecosystems*, 3(1), 41–56, doi:10.1007/s100210000009, 2000.

894 Wang, X., Zhong, S., Bian, X. and Yu, L.: Impact of 2015–2016 El Niño and 2017–
895 2018 La Niña on PM_{2.5} concentrations across China, *Atmos. Environ.*, 208, 61–73,
896 doi:10.1016/J.ATMOSENV.2019.03.035, 2019.

897 Whalen, S. C.: Biogeochemistry of Methane Exchange between Natural Wetlands and
898 the Atmosphere, *Environ. Eng. Sci.*, 22(1), 73–94, doi:10.1089/ees.2005.22.73, 2005.

899 Xu, X., Elias, D. A., Graham, D. E., Phelps, T. J., Carroll, S. L., Wullschleger, S. D. and
900 Thornton, P. E.: A microbial functional group-based module for simulating methane
901 production and consumption: Application to an incubated permafrost soil, *J. Geophys.*
902 *Res. Biogeosciences*, 120(7), 1315–1333, doi:10.1002/2015JG002935, 2015.

903